

## Mid-IR Semiconductor Lasers for Chemical Sensing

Cory J. Hill and Rui Q. Yang

Jet Propulsion Laboratory, California Institute of Technology, Pasadena, CA 91109

Copyright ©2003 Society of Automotive Engineers, Inc

### ABSTRACT

The development of mid-IR semiconductor diode lasers based on type-II interband cascade structures is presented. How these diode lasers can be developed to meet the requirements in chemical sensing applications is discussed.

### INTRODUCTION

Many gases of technological interest exhibit their fundamental absorption lines in the mid-IR (3-12  $\mu\text{m}$ ) wavelength range. Examples of these include  $\text{C}_2\text{H}_2$  (3.07  $\mu\text{m}$ ),  $\text{CH}_4$  (3.3  $\mu\text{m}$ ),  $\text{HCl}$  (3.4  $\mu\text{m}$ ), and  $\text{H}_2\text{CO}$  (3.55  $\mu\text{m}$ ),  $\text{CO}_2$  (4.2  $\mu\text{m}$ ),  $\text{CO}$  (4.6  $\mu\text{m}$ ),  $\text{NO}$  (5.3  $\mu\text{m}$ ), and  $\text{NH}_3$  (6.1  $\mu\text{m}$ ). Hence, the availability of compact and efficient mid-IR semiconductor lasers would dramatically enhance chemical sensing capabilities with significantly improved detection sensitivity. In addition, mid-IR lasers will offer many advantages in terms of cost, volume, weight, design simplicity, reliability, remote sensing capability, fast response, and selectivity. Here we will describe our recent progress in the development of mid-IR semiconductor lasers for chemical sensing. Our approach is based on interband cascade laser structures that utilize optical transitions between the conduction and valence bands in a staircase of Sb-based type-II quantum wells [1] with quantum efficiencies exceeding the conventional limit of unity. By combining the advantages of quantum cascade (QC) lasers [2] and type-II quantum well interband lasers, type-II IC lasers can, in theory [3,4], operate in continuous wave (cw) mode up to room temperature with high output power. Significant advances toward such a high performance level have been reported [5-7] in terms of high peak output power and power conversion efficiency. However, when contrasted with other semiconductor laser technologies such as InP-a nd GaAs-based QC lasers, the amount of effort expended in developing Sb-based IC lasers has been very limited, and their performance is still far from the theoretical projections. Here, we will report the development of Sb-based mid-IR IC lasers for

chemical sensing applications at the Jet Propulsion Laboratory.

### EXPERIMENT

Two IC laser structures with 15 and 23 stages with calculated lasing wavelengths of 3.1 and 3.9  $\mu\text{m}$ , respectively, were grown in a solid source molecular beam epitaxy (MBE) system on unintentionally doped *p*-type GaSb (001) substrates. The IC laser structures are composed of multiple coupled quantum wells (QWs) made from Al(In)Sb, InAs, and Ga(In)Sb layers [5-7]. The total thickness of the MBE-grown layers was near 5  $\mu\text{m}$  for 15-stage structure and about 6  $\mu\text{m}$  for the 23-stage structure. The substrate temperature during growth was maintained at 430°C. The Sb-to-group-III beam-equivalent-pressure (BEP) ratio was ~3:1 and the As-to-group-III BEP ratio was ~15:1. For both samples, many sharp satellite peaks were observed in double-crystal x-ray diffraction (DCXRD) spectra, indicative of their high structural quality. Reciprocal-space scans of asymmetric x-ray peaks revealed no detectable relaxation in the laser structures. After the growth, samples were processed into broad-area gain-guided metal-stripe or mesa-stripe devices with a width of either 100 or 150  $\mu\text{m}$ . Metal contacts were deposited onto the top *n*-type layer and the *p*-type substrate. Laser bars were cleaved to cavities from ~0.7 to 1.5 mm long with both facets left uncoated. The laser bars were affixed with indium, epilayer side up, onto a Cu block and the devices were then wire-bonded to pin-outs connected to the control electronics. The Cu block was then mounted on the temperature-controlled cold finger of an optical cryostat. The optical output power was measured with a cooled InSb detector calibrated by a thermopile power meter when the average power was high. For most measurements, neutral density filters were used to avoid saturating the detector. The emission spectra were obtained by focusing the output optical beam onto the entrance slit of a 0.55-m monochromator.

### RESULTS AND DISCUSSIONS

## A. Gain-Guided Metal-Stripe Lasers

Gain-guided metal stripe (100- $\mu\text{m}$ -wide) lasers made from the 15-stage IC structure sample lased at temperatures up to 130 K and at wavelengths near 2.8  $\mu\text{m}$  as shown in Fig. 1. Long-term variations in MBE growth-rates due to cell depletion led to the actual layer thickness deviating ( $>12\%$ ) from the design, leading to the observed wavelength shorter than the designed value. Hence, the lasers did not perform as expected. Since gain-guided lasers were made simply by depositing metal stripe on the top of contact layer without lateral current confinement, the current spreading is significant and consequently the laser threshold current is large ( $> 1 \text{ A}$ ). The MBE growth rates were recalibrated before growth of the 23-stage structure to bring results closer to design.

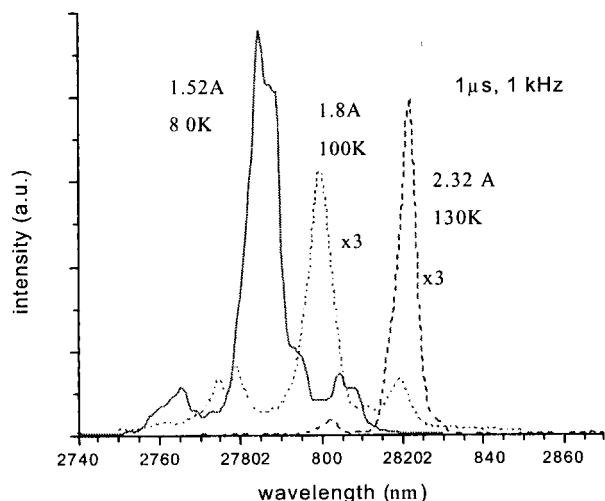
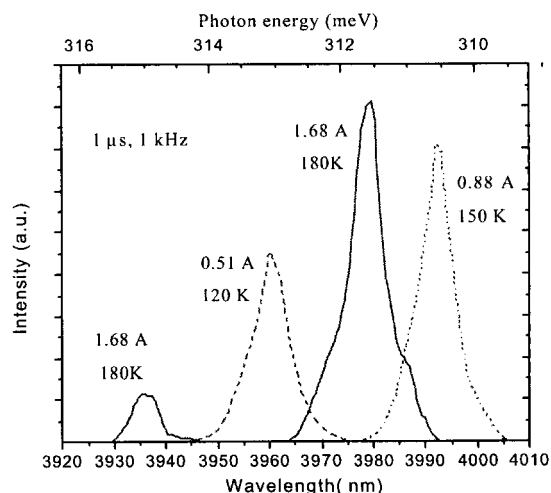


Fig. 1. Lasing spectra of a 15-stage gain-guided 100- $\mu\text{m}$ -wide metal-stripe laser at several temperatures and with 1- $\mu\text{s}$ -long current pulses at 1 kHz.

The gain-guide metal-stripe devices made from 23-stage IC laser structure lased at temperatures up to 200 K and at wavelengths near 4  $\mu\text{m}$  in a good agreement with the design. Their typical lasing spectra are shown in Fig. 2. At 180 K, two major peaks were observed with a separation smaller than 5 meV. Similar behavior was observed from previously reported IC lasers [7]. Although the phenomenon is not yet well understood, it may be indicative of slight difference in emission/absorption spectra from each cascade stage due mainly to a non-identical electric

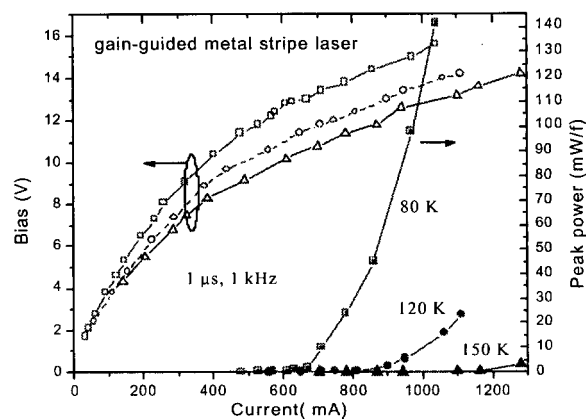
field distribution under large current injection and high voltage conditions, as well as possible variations between cascade stages during the lengthy MBE growth. Also, in comparison to those at 120-150 K, the observed blue shift of the lasing wavelength might be due to the increased band filling and Stark effects from large currents at 180 K operation, or the possible emergence of additional modes at shorter wavelengths.



Quantum efficiencies as high as 400% were observed from these 23-stage IC lasers. A representative current-voltage-light characteristics is shown in Fig. 3, displaying a large peak power ( $>100 \text{ mW}$ ) at 80 K and relatively high threshold bias of  $\sim 13 \text{ V}$  for a gain-guide laser.

Fig. 2. Lasing spectra of a 23-stage gain-guided 100- $\mu\text{m}$ -wide metal-stripe laser at several temperatures and with 1- $\mu\text{s}$ -long current pulses at 1 kHz.

Fig. 3. Current-voltage-light characteristics of a 23-stage gain-guided 100- $\mu\text{m}$ -wide metal-stripe laser at several temperatures and with 1- $\mu\text{s}$ -long current pulses at 1 kHz.



## B. Mesa-Stripe Lasers

To suppress lateral current spreading, mesa structures were formed by chemical etching from the top layer down past the bottom of the cascade stages. Initially, mesa-stripe lasers were made using metal-stripe patterns from the previous gain-guided lasers. However, those 100- $\mu\text{m}$ -wide mesa-stripe lasers were found by SEM analysis to have significant undercut and consequent metal hangover on the edges. Consequently, those lasers were relatively easily damaged or burned under current injection with high voltages. Later, 150- $\mu\text{m}$ -wide mesa-stripe lasers were made with 100- $\mu\text{m}$ -wide metal-strips to eliminate metal undercut. Below, we will describe characteristics of these 150- $\mu\text{m}$ -wide mesa stripe lasers.

Fig. 4 shows the current-voltage-light characteristics of a mesa-stripe (150  $\mu\text{m} \times 0.9 \text{ mm}$ ) laser made from the 15-stage IC structure. This laser exhibited high external quantum efficiency of  $\sim 300\%$  with peak powers exceeding 50 mW/facet. The laser could lase at temperatures up to 230 K before was damaged at 240 K and larger currents. The inset of Fig. 4 shows its lasing spectra in the wavelength range from  $\sim 2.97$  to 3  $\mu\text{m}$ , red shifting when temperature was raised from 200 to 230 K with a rate of  $\sim 0.83 \text{ nm/K}$  (Fig. 5). The threshold current density increased with temperature with a characteristic temperature  $T_0$  of 60 K (Fig. 5) and was lower than what was reported for previous IC lasers at similar wavelengths [8]. The threshold bias was higher than 12 V, resulting in a significant amount of heating and hence the laser could not lase in cw mode at operation temperatures accessible with our measurement setup ( $> 80 \text{ K}$ ).

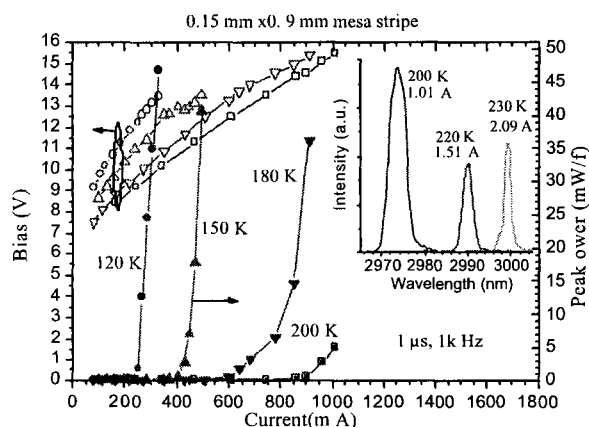


Fig. 4. Current-voltage-light characteristics of a 15-stage mesa-stripe laser at several temperatures and with 1- $\mu\text{s}$ -long current pulses at 1 kHz. The inset shows its lasing spectra.

More systematic spectral measurements of another 15-stage mesa-stripe laser revealed some details of how lasing wavelengths shift with the temperature. This device lased at temperatures up to 235 K. At current levels somewhat above the threshold, there could be two or more emission peaks. At low temperatures ( $T < 180$ ), the peak at the shorter wavelength appeared first when the threshold was reached. However, when the temperature is at 180 K or higher as marked in Fig. 5, the peak at a relatively longer wavelength emerged first. The two groups had a wavelength shift rate ( $d\lambda/dT$ ) of 0.81 nm/K and 0.7 nm/K, respectively, as shown in Fig. 5. This rate is smaller than the band-gap change of the bulk material (e.g. InAs) and the wavelength temperature coefficients for optically pumped type-II QW lasers [9] and type-I QW diode lasers [10]. This is because the Stark effect is more significant with spatially indirect transitions in type-II IC lasers.

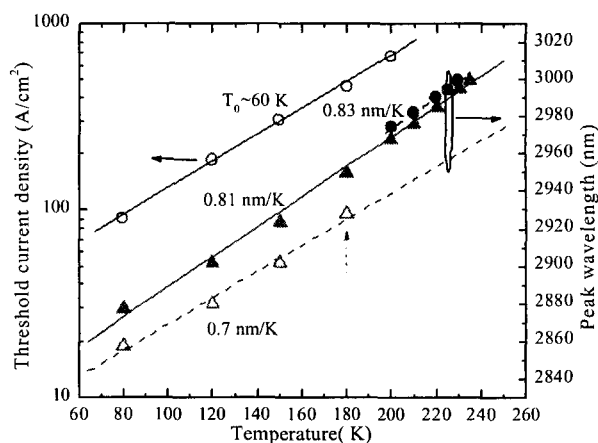


Fig. 5. Threshold current density and the lasing peak wavelength of a 15-stage mesa-stripe laser (circles). The lasing wavelength of another 15-stage mesa-stripe laser (triangles) from the same growth.

Mesa-stripe lasers made from the 23-stage IC structure had significantly reduced threshold current compared to gain-guided lasers and lased at temperatures up to 230 K, the highest reported in the literature for interband diode lasers at this wavelength ( $\sim 4 \mu\text{m}$ ). The threshold current density and threshold bias are shown in Fig. 6 for a 150  $\mu\text{m}$ -wide and 1.2-

mm-long mesa-stripe laser as a function of temperature. Its threshold current density was about  $39 \text{ A/cm}^2$  with a threshold bias of  $\sim 9.2 \text{ V}$  at  $80 \text{ K}$  under pulsed conditions and increased nearly exponentially with a characteristic temperature,  $T_0$ , of  $44 \text{ K}$ . Continuous wave operation was achieved in this mesa-stripe laser at temperatures up to  $100 \text{ K}$  with higher threshold current densities. This is indicative of significant heating. The maximum estimated cw operation temperature of this  $150\text{-}\mu\text{m}$ -wide mesa-stripe laser is about  $110 \text{ K}$  based on the extracted thermal resistance of approximately  $11 \text{ K/W}$  at  $100 \text{ K}$ . Fig. 7 shows its current-voltage-light characteristics at several temperatures with its cw emission spectra shown in the inset. The cw emission spectra at several current levels (just below and above threshold) demonstrate the significant increase ( $\sim 1000$  times) of emission intensities after lasing is achieved. The oscillations in the inset of Fig. 7 indicate constructive and destructive interference of optical modes within the Fabry-Perot cavity. The separation between adjacent longitudinal modes is  $\sim 18 \text{ \AA}$ , in good agreement with the calculated value for a  $1.2\text{-mm}$ -long-Fabry-Perot cavity.

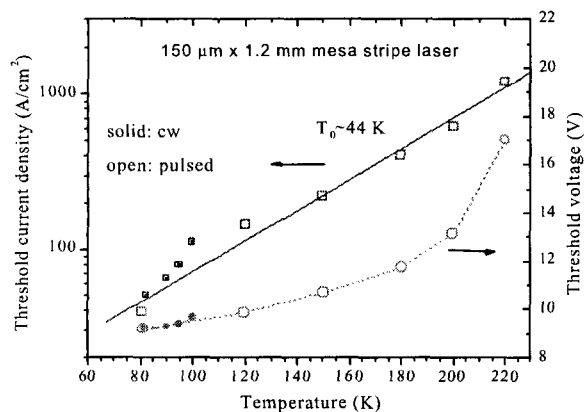
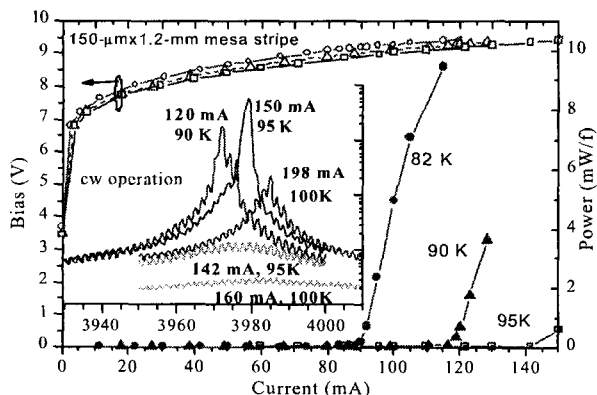


Fig. 6. Threshold current density and bias for a  $150 \mu\text{-m}$ -wide,  $1.2\text{-mm}$ -long mesa-stripe laser as a function



of temperature.

Fig. 7. Current-voltage-light characteristics and cw lasing spectra (inset) at several temperatures for the 23-stage mesa stripe laser.

## LATEST DEVELOPMENTS

By analyzing the characterization results of lasers made from the first sample, we refined the design and grew another 15-stage IC laser sample with well-calibrated MBE growth rates. The sample was processed into  $150 \mu\text{-m}$ -wide and  $0.78 \text{ mm}$ -long mesa stripe lasers. Our preliminary testing has observed above room temperature (up to  $310 \text{ K}$ ) lasing under pulsed conditions. The lasing spectra are plotted in Fig. 8, showing lasing wavelength from  $\sim 3.22$  to  $3.26 \mu\text{m}$  in the temperature range from  $270$  to  $310 \text{ K}$ . The operation temperature is the highest reported for mid-IR interband diode lasers. The laser also lased in cw at temperatures up to  $165 \text{ K}$  as shown in Fig. 9. The cw operation temperature can be raised even higher with use of a narrow-stripe ridge-structure.

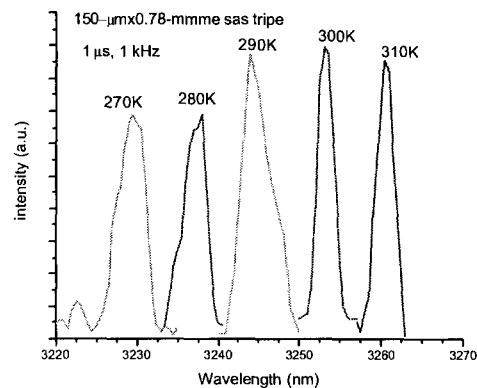


Fig. 8. Pulsed lasing spectra for an improved 15-stage laser growth from  $270$  to  $310 \text{ K}$ .

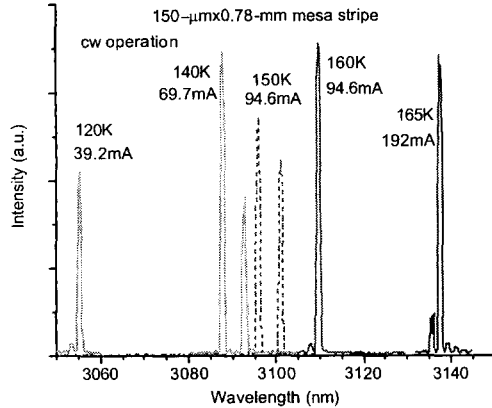


Fig.9. Continuous-wave lasing spectra for an improved 15-stage laser growth from 120 to 165K.

### CONCLUDING REMARKS

Type II IC lasers are still in an incipient stage of their development. They make use one of the least mature III-V materials technologies and the device fabrication process is still in the early stages of optimization. However, with continuing effort and support, the development of this type II IC laser will rapidly progress to the point where the devices will be able to meet the application requirements of chemical sensing and environmental monitoring.

### ACKNOWLEDGMENTS

The authors acknowledge J.K. Liu and B. Yang for their contributions in device processing, and Kenneth C. Evans for SEM analysis. The work was supported by the Jet Propulsion Laboratory, California Institute of Technology, under a contract with the National Aeronautics and Space Administration (NASA).

### REFERENCES

1. R. Q. Yang, "Infrared laser based on intersubband transitions in quantum wells", at *7th Inter. Conf. on Superlattices, Microstructures and Microdevices*, Banff, Canada, August, 1994; *Superlattices and Microstructures*, **17**, 77 (1995).
2. J. Faist, F. Capasso, D. L. Sivco, C. Sirtori, A. L. Hutchinson, and A. Y. Cho, "Quantum Cascade Lasers", *Science* **264**, 553, 1994.
3. J. R. Meyer, I. Vurgaftman, R. Q. Yang, and L. R. Ram-Mohan, "Type-II and type-I interband cascade lasers", *Electronics Letters*, **32**, 45 (1996).
4. I. Vurgaftman, J. R. Meyer, and L. R. Ram-Mohan, "High-power/low-threshold type-II interband cascade mid-IR laser-Design and modeling", *IEEE Photo. Tech. Lett.* **9**, 170 (1997).
5. R. Q. Yang, "Novel concepts for infrared lasers", chapter 2 in *Long Wavelength Infrared Emitters Based on Quantum Wells and Superlattices*, edited by M. Helm (Gordon and Breach, Singapore, 2000), pp. 13-64.
6. R. Q. Yang, "Mid-Infrared Interband Cascade Lasers Based on Type-II Heterostructures", *Microelectronics J.* **30**, 1043 (1999); and references therein.
7. R. Q. Yang, J.L. Bradshaw, J.D. Bruno, J.T. Pham, D.E. Wortman, "Mid-IR type-II interband cascade lasers", *IEEE J. Quantum Electron.* **38**, 559 (2002); and references therein.
8. C. L. Felix, W. W. Bewley, I. Vurgaftman, J. R. Meyer, D. Zhang, C.-H. Lin, R. Q. Yang, and S. S. Pei, "Interband Cascade Laser Emitting > 1 Photon per Injected Electron", *IEEE Photonics Technol. Lett.* **9**, 1433 (1997).
9. W. W. Bewley, C. L. Felix, E. H. Aifer, D. W. Stokes, I. Vurgaftman, L. J. Olafsen, J. R. Meyer, M. J. Yang, and H. Lee, "Thermal characterization of diamond-pressure-bond heat sinking for optically pumped mid-infrared lasers", *IEEE Quantum Electron.* **35**, 1597 (1999).
10. H.K. Choi and G.W. Turner, "Antimonide-Based Mid-Infrared Lasers", chapter 7 in *Long Wavelength Infrared Emitters Based on Quantum Wells and Superlattices*, edited by M. Helm (Gordon and Breach, Singapore, 2000), pp. 225-306.
- 11.